

MOLECULAR DYNAMICS STUDY OF CLUSTER GROWTH AND POLYMER DEGRADATION

Estela Blaisten-Barojas

*Institute for Computational Sciences, Departments of Physics and Chemistry,
George Mason University, Fairfax, Virginia 22030, U.S.A.*

This work is an overview on two molecular dynamics studies of processes at temperatures characteristic of a flame -- growth of silicon clusters from binary cluster collisions and thermal degradation of polymers. In the first study, silicon clusters grow as a consequence of cluster-cluster collisions by forming transient agglomerates that coalesce in a few picoseconds. The collision energy accommodates within the cluster favoring the formation of globular larger clusters regardless of the collision energy and of the impact parameter. On the average the probability for the clusters to stick upon collision is almost 1, showing clearly that the process is irreversible. The second study concerns simple polymeric chains undergoing fragmentation when they burn. These fragments are products of thermal degradation. The consorted sequence of depolymerization reactions arises after fragmentation. As a result, a sample of degrading fragments is formed where the polymer chains have dramatically coiled. These fragments self trap themselves in coiled conformations due to the cooling effect produced by the depolymerization reaction.

1. INTRODUCTION

Recently, numerous innovations in cluster measurements and technologies have led to the discovery of a richness of cluster geometries built up in many by building blocks with magic numbers of atoms.^{1,2} Clusters in the liquid state have also been postulated.³ Physisorption, heterogeneous catalysis, nucleation, fragmentation either thermal or caused by energy or charge instabilities are some of the phenomena that need theoretical support. The validity of a comparison between theoretical predictions and experiments may be sometimes questioned because of the complexity of the experimental interpretation as compared to the simplicity of the theoretical model. Furthermore, the testing of a theoretical prediction may be restricted because of limitations in the experimental state-of-the-art. Computer simulations have added a new scope to scientific research in the rapidly growing field of cluster physics and chemistry⁴ by alleviating these bottlenecks in various areas of physical chemistry. In this work we discuss two selected computer simulations studies of high temperature processes that take place in flames. The first example is developed in Section 2, and concerns the study of the growth of silicon particles in a flame, with special emphasis on the irreversible energy accommodation that occurs in cluster-cluster collisions. The second example is given in Section 3. It describes the thermal degradation of simple polymers by depolymerization reactions that occur during the combustion of the material.

2. COLLISION OF SILICON CLUSTERS. MECHANISM OF ENERGY ACCOMMODATION

The major obstacle to reach the goal of submicron microelectronic features before the end of the century is to control the formation of low vapor pressure solid particles. From the microelectronics scenario, it would be ideal to inhibit the growth of clusters when these have reached a desired size. On the other hand, virtually all ceramic parts start from powder precursors. Therefore, from the scenario of ceramics synthesis, one would like to bias the

growth to obtain desired chemicals and of morphological specimens. In both cases, *how* clusters grow to reach submicron sizes is a relevant issue.

Distributions of cluster sizes displaying magic numbers have been observed in a variety of supersonic jet beam and gas aggregation experiments where vapor equilibrium is established.^{1,2} For manifestly nonequilibrium systems such as flames and aerosols, ordered or structured distributions of sizes are not predominant.⁴⁻⁹ In this study we were motivated by the cluster and particle formation that occurs in counter-propagating diffusion flame reactors.^{5,6} In a flame environment, the growth of particles may proceed by simple monomer addition to a pre-formed cluster, or may be influenced by the coalescence of colliding clusters. The distribution of particle sizes depends strongly on the energy dissipation that follows cluster-cluster collisions. Modeling efforts have tried to account for both modes of growth within a kinetic scheme derived from a master equation approach. Nucleation kinetics models consider the small cluster size regime.⁸ Coagulation considers the large particle size regime.⁹ Attempts to model the kinetics of the full spectrum of cluster sizes (molecules, clusters, and particles)^{5,7} exist also. Growth being essentially an irreversible process, all of these models make the common assumption that growth rates occur at the cluster collision rate. That is, the sticking coefficient is unity no matter the size or composition of the species undergoing collisions. These approaches cannot account for chemical composition changes, energy dissipation, evaporation, or molecular level dynamics occurring in the picosecond scale. As such, these models are limited to gross calculations of growth rates.

In the following paragraphs we describe a molecular dynamics study of the initial steps of cluster growth due to cluster-cluster collisions. The computer experiment was designed to consider collisions of silicon clusters and the purpose of the simulation was to test the validity of the kinetic assumption. Silicon was chosen because of its obvious practical importance to the microelectronics community. Silicon clusters are also formed in counterpropagating diffusion flame reactors as a byproduct of the production of silica.^{5,6} In that process clusters and particles grow from a hydrogen-oxygen flame when the hydrogen stream is doped with small quantities of silane. Our simulation was motivated by the observed changes in the distribution of particle sizes detected in those experiments as a function of time.

2.1 Model and Methodology

Silicon clusters at temperatures characteristic of a flame were modeled using Stillinger-Weber¹⁰ potential. This potential contains seven parameters. It correctly describes the bulk melting temperature and structural characteristics of the melt. This potential models the binding energy of each cluster as a sum of 2- and 3-body contributions. Pair potentials alone are insufficient to study covalent materials and to simulate correctly their thermodynamic behavior.¹¹

A pair of colliding clusters are assumed to be immersed in a gaseous fluid formed by atoms and other clusters moving along the streamline of a flame laminar flow at about 2000K. The particle diffusion in the fluid transport of mass equation is fairly constant in time.⁵ Locally, atoms and composition-changing clusters undergo brownian motions. Therefore, from an atomic point of view, the overall stream velocity can be neglected as compared to the brownian velocity which characterizes the temperature of the flame. In this simulation we have simplified the background for each binary cluster collision by replacing it with an average collision energy of 2200K. No energy dissipation towards the bath was considered since the simulation aimed to analyze the short time processes after the collision event.

Molecular dynamics was used throughout to solve Newton's equations of motion.¹¹ Units of length, energy, and time were chosen to be $\sigma = 2.0951\text{\AA}$, $\varepsilon = 2.167\text{ eV}$ and $\tau = 0.072\text{ ps}$. A time step of $5.36 \times 10^{-4}\text{ ps}$ was used. All simulations runs were started from two separated clusters each one containing 15 silicon atoms, and each one aged¹² to bring it into

thermodynamic equilibrium at about 1850K. Prior to collision, the atoms within each cluster are very mobile, and the overall shape of the cluster is continuously changing in time. We have analyzed this cluster size in the past (Figs. 2,7 and 9 of reference 11). At 1850K the pair correlation function has lost all structure indicating that the colliding cluster is liquid-like. Furthermore, the distribution of bond angles peaks towards values lower than the characteristic 109.5° indicating a more compact structures than in the solid phase. The coordination number at the working temperature is about six, in agreement with the fact that liquid silicon is denser than its solid phases. Trajectories were calculated in the center of mass frame. Only head on collisions at various impact parameters were considered. The collision energy was given instantaneously. The collision event commences at $t=0$ with two clusters previously equilibrated at 1850K situated far apart to ensure no interaction among them. The two clusters start moving toward one another with a uniform relative velocity of 506 m/s, consistent with a local brownian motion at 2200K.

2.2 How the Collision Energy is Accommodated.

When the two clusters come into the interaction range of the potential they are accelerated one towards the other. It is at the onset of the collision, when one or a few atom-atom interactions are effective, that the specifics of the model potential becomes dominant. Initially the pairwise attractive forces dominate over the scarce 3-body repulsive contributions. But when the clusters get closer, many more atoms participate in the process, in such a consorted way that 3-body repulsive, and 2-body compressed contributions add up to an instantaneous repulsion that separates the colliding clusters away from each other. However, this instantaneous repulsion is not strong enough as to bring the clusters apart. Instead, the two clusters stick and start an oscillatory relative motion. During this relative oscillation motion the newly formed aggregate behaves as an *agglomerate*, i. e., each one of the two initial clusters keeps its individuality.¹¹ As time evolves the agglomerate fuses giving rise to a larger stable cluster that bears liquid-like properties. Similar cluster aggregation has been reported for solid Lennard Jones clusters.¹³ We have also performed some simulations where the initial temperature of the clusters is about 900 K. In this case the agglomerate is formed very smoothly, and the system remains in this stage for at least 30 ps.

Consider the trajectory along one typical reactive collision at zero impact parameter. Let us call *harpooning time* the time elapsed between the moment at which the first two atoms come into the range of interaction of the potential, and the moment at which the two clusters coalesce. Fig. 1 illustrates the changes along the trajectory that various relevant quantities undergo during the harpooning time. The clusters first touch at about $t=1.5 \tau$. Subsequently the clusters stick oscillating, the new aggregate looks like an agglomerate. Later the agglomerate fuses into one single larger specimen. Oscillations of the relative velocity (Fig 1a) during harpooning gradually go to zero when the harpooning event ends and the two clusters coalesce. The instantaneous changes of the number of bonds in the agglomerate is plotted in Fig. 1b. Two atoms were considered to form a bond if their instantaneous interatomic distance was less than 2.94 Å. Despite the erratic time variations of the number of bonds, both during harpooning and later on, its average remains about the same. **Collisions were almost always completely inelastic** (or reactive). There was sticking in 99.7% of the trajectories analyzed up to now. The non-sticking cases (non-reactive collisions) resulted from grazing collisions at large impact parameters. Figs. 1c and 1d show the distribution of energy during harpooning. Note that the sharp drop in the average potential energy when the clusters first touch is mirrored by an increase in the temperature. At this point the agglomerate is formed. The agglomerate is a transient complex with very short lifetime that lives only while the collision energy is redistributed among the internal vibrations of the new cluster. In time, the system actually goes through a barrier of about 8 kcal/mole before the agglomerate starts its fusion. Fig 1c. shows how fast the potential energy reaches a maximum and declines at a slower pace when the harpooning time is over. Correspondingly, Fig. 1d shows the transient decrease of the temperature that stabilizes the agglomerate, followed by a progressive temperature increase that fuses the agglomerate.

If the clusters would have collided elastically they would have come apart after the harpooning time, carrying away all the collision energy. In these inelastic collisions, the external energy accommodates quite interestingly. Figs. 2a-d illustrate the quantities drawn in Fig. 2, now plotted in a longer time scale. In Fig. 2a it is seen that the relative velocity fluctuates around zero. The plot shows that after the harpooning time, the conversion of collision energy into internal energy is fully accomplished in about 5ps. Fig. 2b shows the fast time variations of the instantaneous number of bonds and the slight increase of its average with time. As the cluster ages, the coalescing agglomerate gains a substantial conformational energy, it self-heats and fuses. This mechanism is responsible for the further decline in potential energy beyond $t=1$ ps and consequent rise in temperature to $T \sim 2300$ K (Figs. 2c-d). On the average, the Si_{30} clusters are capable to accommodate 40 kcal/mole, a large energy for

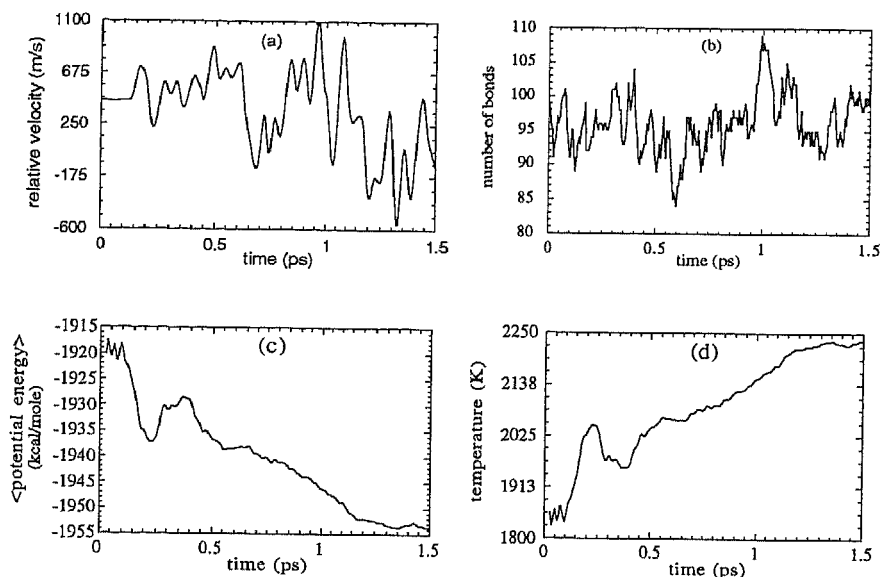


Fig. 1. The oscillatory mode of one collision event. (a) Relative velocity of the colliding clusters; (b) Instantaneous values of the number of bonds in the new agglomerate; (c) Average potential energy of the agglomerate; (d) Temperature of the agglomerate. All quantities are plotted as a function of time.

such small clusters. The temperature of the new single cluster has increased by about 400K, consistent with 60 -70% of the accommodation energy. The collision energy was equivalent to only 10% of the total increase in temperature. The extra increase in the temperature of the cluster is due to the heat of formation of new bonds released in the formation of the coalesced cluster. About 10 new nearest neighbor interactions (bonds) were formed in the coalesced cluster. However the system consumes energy to arrange these bonds in their best orientations yielding a decrease in potential energy of only 1.5 times the energy of a bond (or of a dimer). The increase in the temperature helps this process such that the system accesses energetically favorable conformations in configuration space.¹²

In Fig. 3 are shown nine snapshots along a typical trajectory that begins at $t=0$ while the clusters are well separated. Subsequent photographs are spaced by approximately half of a picosecond, except for the last one that pictures the configuration at $t= 6.5$ ps. The sequence of snapshots shows how the clusters stick together forming the agglomerate during harpooning time, and further how this entity fuses into a single rather spherical cluster.

This accommodation of energy accompanied by the overall heating of the unified cluster is an example of an irreversible conversion of the collision kinetic energy. It would take the age of the universe to concentrate all the collision kinetic energy back into one degree of freedom (the relative motion). The collision kinetic energy was totally dissipated into the 84 internal vibrations and 3 rotations.

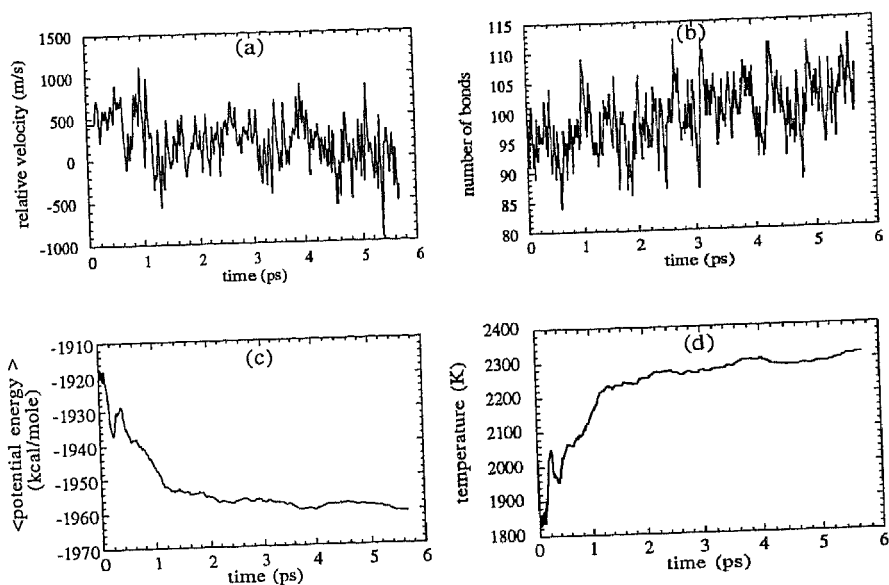


Fig. 2 The collision event after coalescence of the colliding clusters. (a) Relative velocity of the colliding clusters; (b) Instantaneous values of the number of bonds in the new cluster; (c) Average potential energy of the united cluster; (d) Temperature of the united new cluster. All quantities are plotted as a function of time.

2.3 Discussion

Intermolecular forces have long been acknowledged to be of importance in atomic and molecular collisions and therefore in the equations of state of real gases. The question of accommodation in particle collisions must be addressed as a prelude to the discussion of the role of the attractive contribution of interatomic forces.

Let us assume that we are dealing with a gas of atoms. The implications of the intermolecular potential for gas-phase atomic collisions can be treated qualitatively by determining the distance of separation r_{enh} between atoms at which the potential is equal to the thermal energy $k_B T$. This distance is to be compared with σ , the pair potential hard core radius. The ratio r_{enh}/σ is a qualitative measure of the enhancement of the collision radius due to the attractive part of the potential. The corresponding enhancement of the collision cross section is $(r_{\text{enh}}/\sigma)^2$. The enhancement ratio of thermal capture in our case is 2 per pair of atoms.

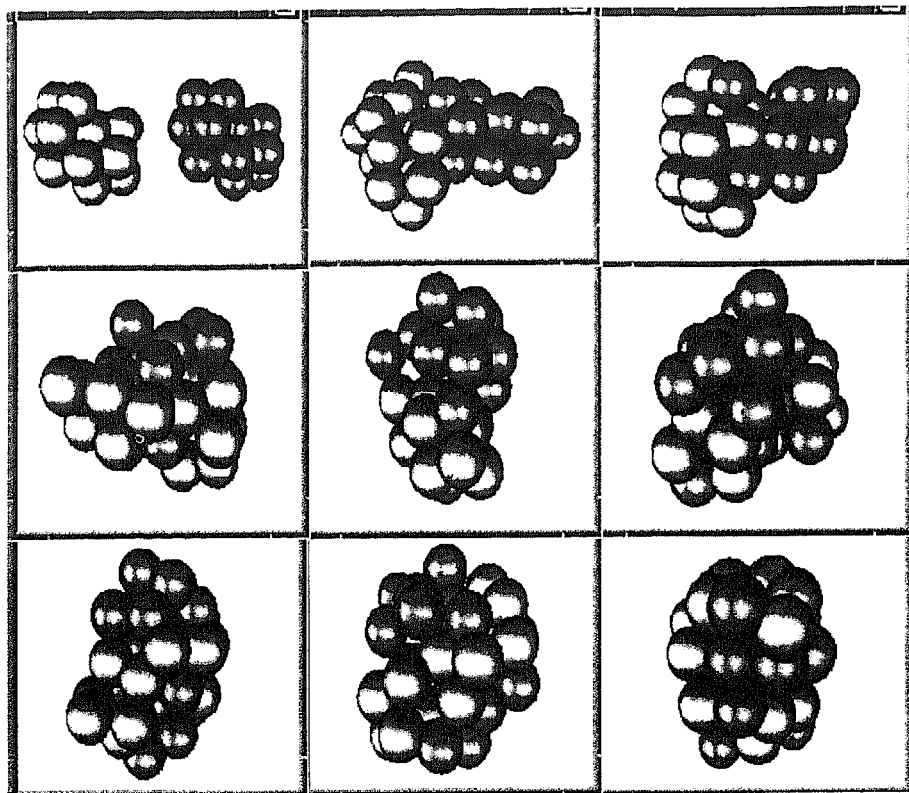
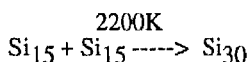


Fig. 3 Snapshots along a typical trajectory. From right to left and top to bottom clusters at $t=0$, $t=0.5\text{ps}$, $t=1\text{ps}$, $t=1.5\text{ps}$, $t=2\text{ps}$, $t=3\text{ps}$, $t=4\text{ps}$, $t=5\text{ps}$, $t=6.5\text{ps}$. Light and dark shades indicate atoms that initiated the trajectory in different clusters. The diameter of the spheres equals 1.4σ .

In collisions of clusters the logistics is less clear. Substantial experimental evidence exists that the collision rates of submicron particles exceed those calculated on the basis of brownian motion of clusters modeled as billiard balls.¹⁴ The estimates yield collision rate enhancements inversely related to the size of the colliding clusters. This statement needs microscopic proof. From our observations, we can state that the thermal enhancement on the capture is very important for Si_{15} . For our clusters with coordination number of about 6, the number of pairs contributing to the thermal capture is about 60. Therefore, the enhancement of the sticking probability is 60 times larger than in a collision of atoms. Moreover, the silicon melt is denser than its various solid phases and the coordination number larger at high temperatures. Thus, sticking by cluster-cluster collision is more effective, and further enhanced when the silicon clusters are melted.

The results in this work show that microscopic reversibility does not apply to cluster collisions. Thus,



is an irreversible reaction. The complete energy accommodation, supplemented by the overall heating, proves it. These cluster-cluster collisions are completely inelastic, in contrast to the frequent hypothesis of microscopic reversibility assumed in molecular collisions of either molecules or solid surfaces. Similar observations were obtained for silicon clusters at about 1000K and are in agreement with simulations of Lennard Jones clusters.¹³ The present work points out how the condensed phases, unified clusters, grow dynamically as a natural consequence of the atom-atom interactions and state variables appropriate to the cluster-cluster collisions. Finally, when the process is accelerated by input of a collision energy equivalent to 10,000 K, the colliding clusters coalesce but never scatter like billiard balls. Rather these unified hot specimens start to evaporate single atoms. This is another proof of the irreversibility of the reaction.¹²

3 COILING AND DEPOLYMERIZATION IN SIMPLE POLYMERS

In the process of combustion, polymeric materials undergo many complex reactions that lead to their thermal degradation with formation of volatile monomers and condensed phase fragments. Once formed, these monomers react with oxygen in the gas phase releasing large amounts of heat in the process of forming stable combustion products. Some of these products are particles on the nanometer scale that result from incomplete depolymerization of the degrading materials. Little is known about the processes leading to the formation of these particles, and a better understanding on these lines is of great interest for the material fabrication. Polymers with a strong tendency to depolymerize are polystyrene, poly (methyl methacrylate), and polytetrafluoroethylene. Several computer models based on both kinetic and statistical approaches have been used to study aspects of the thermal decomposition of polymers.¹⁵⁻¹⁹ We describe in this section a novel computer model of the effects in polyolefines and related polymers caused by the depolymerization reaction.²⁰ The goal is to provide insight into the mechanisms leading to changes in internal energy and conformation of the degrading polymer fragments.

Depolymerization is a chain reaction which is initiated with the formation of free radical polymer fragments (frp) resulting from the random scission of the original polymer molecules. Depolymerization starts when one monomer dissociates from the end of a frp fragment. The reaction leaves behind a new frp fragment which is reduced in size by one monomer unit.²¹ Subsequently, the newly formed frp fragment ejects a second monomer from its end and, in turn, a smaller frp fragment is left behind. In principle, depolymerization can continue until the initial frp fragments have completely *unzipped* into their component monomers. The unzipping process also terminates when the fragment internal energy is low enough not to support further bond dissociations.

When degradation begins, the condensed material is not in thermodynamic equilibrium, temperatures are high, and depolymerization is triggered. The products of degradation go into the gas phase where the monomers react with oxygen activating the combustion mechanism. It is unclear though why most burning polyolefins give rise to nanometer-particles that mainly degrade into graphitic-like globules that remain suspended in the external atmosphere. It is also unclear why these materials do not volatilize completely, but leave condensed amorphous remnants upon burning. These are some of the many processes that can occur during degradation.¹⁵ At temperatures far below the degradation temperature, these materials are disordered with respect to both the conformation of the individual chains and the chain molecular weights.^{18,19} These polymers are never 100% crystalline, but rather they contain

many coiled chains giving rise to void-like defects. This is because the interactions between polymer chains are weaker than the interactions within each chain. As an initial effort, in this work we concentrate on the effect of the depolymerization reaction on the conformation of each polymeric chain in the material. Thus, chains are considered to be long and to have large molecular weight, but their interaction with the surroundings is not taken into consideration.

Hydrogen transfer reactions and other reaction channels may also participate in the degradation process. But the activation energy for depolymerization is lower than that for other reactions and ultimately depolymerization dominates in most hydrogen-poor polymers. It turns out that less energy is required to initiate depolymerization of a fragment than to produce further random scission, the reduction being the energy difference between a double and a single bond along the backbone. In this work we have only taken into account two possible reaction channels -- thermal random scission and depolymerization. It is observed that polymer fragments undergoing depolymerization result in highly coiled incipient *globules* that cool while depolymerizing. The cooling mechanism competes with depolymerization and eventually terminates the depolymerization process giving rise to long lived colder globules. This behavior contrasts with the polymer fragments resulting from thermal random scission which are extended (not too coiled) and hot.

3.1 Polymer Fragmentation

The molecular dynamics trajectories were initiated from independent polymer chains in free space. The molecular weights of the polymers ranged from 50 M to 950 M, where M is a polymer unit with a mass of 14.5 au (the mass of a CH₂ group). A single polymer chain was represented by *N* spherical units interacting through the classical model potential:

$$V = \sum_{i=1}^{N-1} V_b(r_{i,i+1}) + \sum_{i=1}^{N-2} V_a(\theta_{i,i+1,i+2}) + \sum_{i=1}^{N-2} \sum_{j=i+2}^N V_{nb}(r_{i,j}), \quad (1)$$

Here the first term

$$V_b = D[1 - \exp(-\alpha(r - r_e))]^2, \quad (2)$$

is a Morse potential representing the covalent bond between pairs of adjacent units. The second term is a three-body interaction that favors the angle $\theta_0 = 113.3^\circ$ between any three contiguous units along a zigzag chain consistent with sp³-hybridization:

$$V_a = \frac{1}{2} k_\theta (\cos \theta - \cos \theta_0)^2, \quad (3)$$

The third term is a van der Waals interaction between non-bonded units in the chain:

$$V_{nb} = 2\varepsilon [(\sigma/r)^9 - 1.5(\sigma/r)^6], \quad (4)$$

where the core parameter σ takes into account the excluded volume of the units. Values of the six parameters used to study the torsional motions in butane²² were adopted in this work and their values are reported elsewhere.^{20,23} The global minimum of the potential energy function corresponds to the planar zigzag configuration where all dihedral angles are 180°. The bending

force constant k_θ is large enough to ensure the stability of chains in many different coiled conformations with randomized dihedral angles.

The time evolution of each polymer chain was followed using molecular dynamics at constant energy. The Hamiltonian of each chain was considered to be the sum of the kinetic energy of each unit as a whole plus the potential energy given in Eq. 1. The equations of motion were solved by means of a variable time step predictor-corrector algorithm that controls the local error.²⁴ The maximum time step used was 0.004 ps, which is one order of magnitude smaller than the vibrational period of the covalent bonds. Simulations were always started from the planar zigzag geometry and the initial momenta chosen at random from a uniform distribution. The time evolution of most chains was followed for 10ps. Temperature was defined as $2/3k_B$ times the average kinetic energy per unit.

Each polymer chain was heated instantaneously by an external energy of the order of 0.019 Hartrees/unit. This energy distributed among all degrees of freedom resulting in a Boltzmann distribution of speeds in less than 0.1ps.²³ The chains equilibrated to temperatures in the range of 2500K. Free radical polymer fragments began to form after approximately 1ps by random scission of the original chains. A fragment was formed whenever the distance between neighboring units exceeded $r_d = 18$ au.

Monomers consisted of two units connected by a double bond. The double bond was represented by the Morse potential in Eq. (3), where D was replaced by $D' = 1.759D$. The sequence of reactions leading to depolymerization was simulated by introducing a switching function to modify the pair potential terms V_b on either side of the dissociating bond. Thus, the two bonds adjacent to the dissociating bond were strengthened by the amount $D' - D$ whereas the two next nearest bonds were weakened by the same amount of energy. On the average monomers were ejected every 2ps. At the end of an experiment *both* frp fragments and monomers were present in the fluid.

3.2 Degradation due to Polymer Depolymerization

Thermal random scission of 25 polymer chains, with an average chain length of 478 units, resulted in the formation of 72 frp fragments. Typically chains broke into three or four fragments. The distribution of fractional sizes (ratio of the fragment size to the initial size of the polymer chain) of these fragments is plotted in Fig. 4. This bimodal distribution is not simple because the number of random scissions was not the same for all experiments. The noticeable bias towards small fractional sizes is consistent with statistical predictions based on discrete breakage models,²⁵ but it disagrees with the log-normal distributions resulting from liquid-like coalescence of particles.²⁶

The degree of coiling was measured by the average radius of each frp fragment :

$$\langle r \rangle = \sum_{i=1}^n |\vec{r}_i - \vec{r}_0| / N, \quad (5)$$

where \vec{r}_i is the position vector of the i 'th atom, and \vec{r}_0 is the position vector of the center of mass of the fragment. The degree of coiling in a fragment is inversely related to the average radius²⁷ (the average radius of a coiled fragment is small compared to a planar zigzag chain containing the same number of units). These radii are plotted in Fig. 5 as a function of the number of units in the frp fragments. Fig. 5a is a plot of data corresponding to fragments that *did not* depolymerize, and Fig. 5b collects the data of fragments that *did* depolymerize. Solid lines in Figs. 5a,b correspond to perfect planar zigzag polymers. We observed that the ejection

of monomers was followed by a recoil which, after many such reactions, resulted in a compression of the depolymerizing fragments. The dihedral angles in the fragments randomized in the process producing coiled fragments. Comparison of Figs. 5a and b indicates

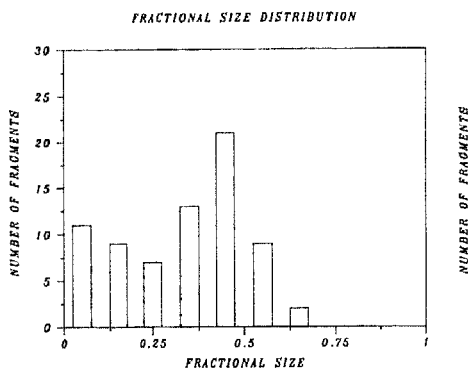


Fig. 4 Distribution of fractional sizes from 72 polymer fragments. Fractional sizes were defined as the ratio of the number of units in the fragment to the number of units in the original polymer prior to fragmentation

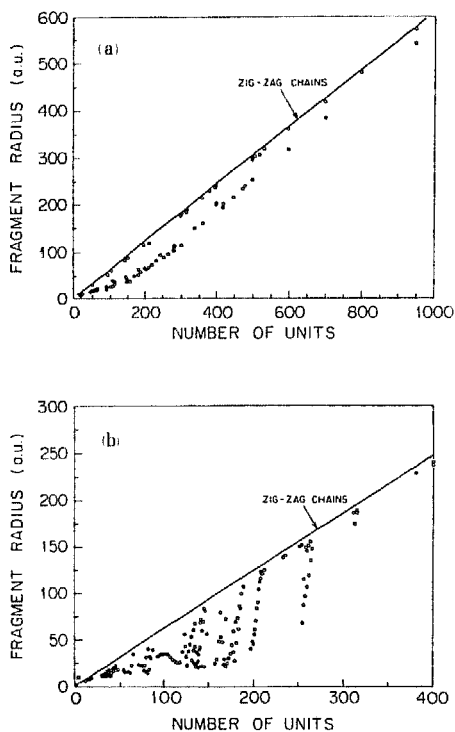


Fig. 5 Average radii of free radical fragments as a function of the number of units. (a) Fragments that did not depolymerize; (b) fragments that depolymerized. The straight line corresponds to perfect planar zigzag polymers.

that coiling is substantially enhanced in the depolymerizing fragments. The radii of the fragments that did not depolymerize decreased by about 20 % from their planar zigzag values, whereas the radii of depolymerizing fragments typically decreased by more than 50%. Highly coiled, depolymerizing fragments looked like *globules* (spherical molten polymer particles). The dramatic shrinkage in size is clearly visible in computer videos based on the trajectories of the degrading polymer fragments.²⁸

Globules presented a tendency to cool in the process of depolymerizing. In contrast, the stretched fragments that did not depolymerize tended to maintain their original temperature. Internal cooling is a consequence of the rapid succession of bond dissociations to eject the monomers. As an illustration, one 36-unit coiled fragment in the process of depolymerizing at $T = 1700\text{K}$ was collected at $t = 16.5\text{ps}$ along a typical trajectory and depicted in Fig. 6. Also is the plot of the temperature changes of the parent fragment as a function of the number of its remaining units. The ability to self cool tended to inhibit further depolymerization by trapping the free radical inside the coils. As a result the lifetime of the coiled fragments was noticeably increased. *The fragments self quenched in melted-like conformations.*

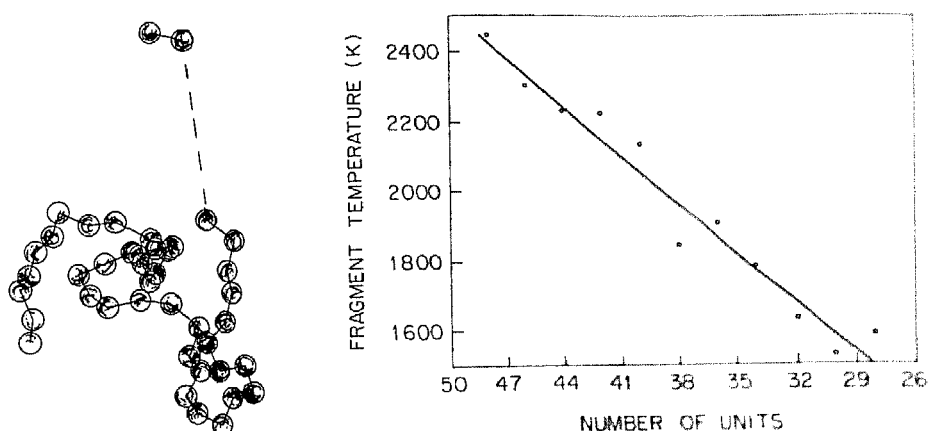


Fig. 6 A depolymerizing fragment and the changes of the internal temperature as a function of the remaining number of units.

Other qualitative observations worth noting concern the infrared spectrum as obtained from the Fourier transform of the velocity autocorrelation function which is depicted in Fig. 7. This spectrum corresponds to a sample of 4 frp fragments that started to depolymerize at a temperature of 2100K . The main spectral features are two broad bands centered at about 1000 and 150 cm^{-1} , plus an intense peak at very low frequencies. The broad high frequency band corresponds to the stretching vibrations of the individual unit-unit bonds. Broadening is due to the many different neighborhoods of dihedral angles near each unit-unit bond. The second band corresponds primarily to acoustic-like vibrations in which many units move in phase along the coiled polymer backbone. The intensity of this band, relative to the high frequency band, showed a tendency to increase with time. This would suggest that IR spectra taken as a function of time is a possible tool to detect the extent of fragments that became globular. The peak at very low frequencies is due to the rotation of the independent fragments as a whole, to the rotation of the individual monomers, to the vibrations between the dissociated monomers, to the vibrations between the dissociated monomers and the polymer fragments, and to the vibrations between different polymer fragments.

Our observations help to understand why complete depolymerization is hard to achieve and how complex particles might be formed along with monomers at the moment of the combustion.

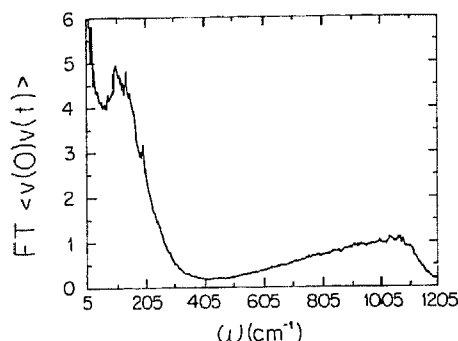


Fig. 7 Fourier transform of the velocity autocorrelation function (x component) of a 400-unit polymer undergoing depolymerization. After 10ps, four frp fragments and 22 monomers were present in the sample.

ACKNOWLEDGMENTS

This work was supported by the National Science Foundation under grant RII-8902850, and by the Process Measurements Division and the Fire Measurement & Research Division of the National Institute of Standards and Technology.

REFERENCES

1. For a starting point into this literature see: "Proceedings of Faraday Symposium on Large Gas Phase Clusters", J. Chem. Soc. Faraday Trans., **86** (1990).
2. "Elemental and Molecular Clusters", Benedek G., Martin T. P., and Pacchioni G., editors, Monographs on Material Science Vol. 6, Springer-Verlag, Berlin, Heidelberg, New York (1988).
3. Blaisten-Barojas E., Garzon I. L., and Avalos Borja M., in "Large Finite Systems", Jortner J., Pullman A., and Pullman B., editors, Reidel, Boston (1987); *ibid.*, Phys. Rev. B., **40**, 4749 (1989).
4. Marlow W. H., in "Aerosol Microphysics I: Particle Interaction", Springer-Verlag, Berlin, Heidelberg, New York (1980).
5. Zachariah M. R. and Semerjian H. G., *AIChE J.* **35**, 2003 (1989).
6. Chung S. L. and Katz J. L., *Combust. Flame* **61**, 271 (1985).
7. Gelbard F., Tambour Y., and Seinfeld J. H., *J. Colloid Interface Sci.* **76**, 541 (1980).
8. Bauer S. H. and Frurip D. J., *J. Phys. Chem.* **81**, 1015 (1977).
9. Dobbins R. A. and Mulholland G. W., *Combust. Sci. Technol.* **40**, 175 (1985).
10. Stillinger F. H. and Weber T. A., *Phys. Rev. B* **31**, 5262 (1985).
11. Blaisten-Barojas E. and Levesque D., *Phys. Rev. B* **34**, 3910 (1986).
12. Blaisten-Barojas E. and Zachariah R. M., *Phys. Rev. B* **45**, 4403 (1992).
13. Gay J. G. and Berne B. J., *J. Colloid Interface Sci.* **109**, 90 (1986).
14. Okuyama K., Kousaka Y., and Hayashi K., *J. Colloid Interface Sci.* **101**, 98 (1984).
15. Mita I, Chap. 6, in "Aspects of Degradation and Stabilization of Polymers", Jellinek H. H. G., ed., Elsevier, Amsterdam, (1978).
16. Guaita M., Chiantore O., and Costa L., *Poly. Deg. and Stab.* **12**, 315 (1985).

17. Inaba A., Kashiwagi T., and Brown J. E., *Poly. Deg. and Stab.* 21, 1 (1988).
18. Rigby D. and Roe R. J., *J. Chem. Phys.* 87, 7285 (1987).
19. Noid D. W., Pfeffer G. A., Cheng S. Z. D., and Wunderlich B., *Macromolecules* 21, 3482 (1988).
20. Blaisten-Barojas E. and Nyden M. R., *Chem. Phys. Lett.* 171, 499 (1990).
21. Sumpter B. G. F. and Thomson D. L., *J. Chem. Phys.* 88, 6889 (1988).
22. Weber T. A., *J. Chem. Phys.* 70, 4277 (1979).
23. Nyden M. R. and Noid D. W., *J. Phys. Chem.* 95, 914 (1991).
24. Shampine L. F. and Gordon M. K., "Computer Solution of Ordinary Differential Equations", Freeman, San Francisco (1975).
25. Zahedi H. and Shapiro S. S., *Commun. Statist. Theory Meth.* 18, 199 (1989).
26. Granqvist C. G. and Buhran R. A., *J. Appl. Phys.* 47, 2200 (1976).
27. Flory P. J., "Principles of Polymer Chemistry", Cornell University Press, Ithaca (1957).
28. Nyden M. R. and Blaisten-Barojas E., video-material (available from the authors).